View metadata, citation and similar papers at core.ac.uk
brought to you by CORE
provided by Open Repository and Bibliography - Luxembourg

23rd Nordic Seminar on Computational Mechanics
NSCM-23
A. Eriksson and G. Tibert (Eds)
©KTH, Stockholm, 2010

INFLUENCE OF PISTON DISPLACEMENT ON THE SCAVENGING AND SWIRLING FLOW IN TWO-STROKE DIESEL ENGINES

A. OBEIDAT[†], S. HAIDER,[†] K. M. INGVORSEN [†], K. E. MEYER[†], AND J. H. WALTHER [†]

[†]Department of Mechanical Engineering
Technical University of Denmark
DK-2800 Kgs. Lyngby, Denmark
Tel.: +45-4525 4327
Fax: +45-4588 4325

Key words: diesel engine, swirl, scavenging, LES simulation.

Summary. We study the effect of piston motion on the in-cylinder swirling flow in a low speed, large two-stroke marine diesel engine. The work involves experimental, and numerical simulation using OpenFOAM platform, Large Eddy Simulation was used with three different models, One equation Eddy, Dynamic One equation Eddy, and Ta Phouc Loc model, to study the transient phenomena of the flow. The results are conducted at six cross sectional planes along the axis of the cylinder and with the piston displaced at four fixed piston positions covering the air intake ports by 0%,25%, 50%, and 75% respectively, for the fully opened case LES model with 8/12 million mesh points were used. We find that the flow inside the cylinder changes as the ports are closing, from a Rankine/Burger vortex profile to a solid body rotation while the axial velocity profiles change from a wake-like to a jet-like profile.

1 INTRODUCTION

In two stroke engines, compared to 4-stroke engines, the removal of exhaust gases and supply of fresh air for the next cycle is carried out simultaneously using the scavenging process. Scavenging is carried out using air entering the cylinder from intake ports at the cylinder liner walls near the bottom dead centre and scavenging the exhaust gases from cylinder through the exhaust port. The scavenging process removes the exhaust gases, provides fresh air to the engine , and provides the necessary swirl to the flow in which the diesel fuel is to be injected. This makes the scavenging process very important for engine performance and efficiency both in terms of fuel consumption and emissions. Swirling flows are widely used in industrial applications e.g. cyclone separators, swirl combustors etc. Previous studies [1 2 3] involve swirl generators using guide vanes that divert the radially incoming flow and impart the tangential component. In the present study we focus on the swirling flow in the presence of an obstructing piston and the resulting in-cylinder confined swirling flow.

2 NUMERICAL METHODS

2.1 LARGE EDDY SIMULATION

We study the swirling flow numerically using large eddy simulations. The governing equation are the spatially filtered Navier-Stokes equations:

$$\frac{\partial \bar{u}_j}{\partial x_j} = 0 \tag{1}$$

$$\frac{\partial \bar{u}_i}{\partial t} + \frac{\partial \bar{u}_i \bar{u}_j}{\partial x_j} = -\frac{1}{\rho}\frac{\partial \bar{p}}{\partial x_i} + \nu \frac{\partial^2 \bar{u}_i}{\partial x_j^2} - \frac{\partial \tau^{SGS_{ij}}}{\partial x_j} \tag{2}$$

$$\tau_{ij} = \bar{\rho}\widetilde{u_i u_j} - \bar{\rho}\tilde{u}_i\tilde{u}_j \tag{3}$$

where t denotes the time, u_i is the velocity component in Cartesian coordinates, ρ is the density, p is the pressure, and ν is the kinematic viscosity. As a result of the spatial filtering the subgrid-scale-stresses (SGS) stress tensor $\tau^{SGS_{ij}}$ is introduced into the momentum eq. (2), where $\tau_i^{SGS_{ij}}{}_j = \overline{u_i u_j} - \bar{u}_i\bar{u}_j$.[5 6 7 8 9 10 11]

We apply three different models. The one equation eddy model where the kinetic energy k is solved while another scale is estimated, so if the k is solved then the turbulent velocity u is estimated by $u^* \sim \sqrt{k}$[5]. Eddy viscosity $\mu_i = C_\mu \bar{\rho} k^{\frac{1}{2}} l^*$, where C_μ is a constant, l^* is the turbulent length scale.
The dynamic k-equation eddy-viscosity model, where the model constants are recalculated during the simulation rather than to be pre-calculated, the model stress tensor eq. (3)[12] which can be modeled as

$$\tau_{ij} - \frac{1}{3}\delta_{ij}\tau_{kk} = C\alpha_{ij} \quad C = \frac{L_{ij}M_{ij}}{M_{kl}M_{kl}} \tag{4}$$

where C is the model parameter, M_{ij} is the minimum error, L_{ij} is a stress resolved tensor. α_{ij} is the term needed to be modeled.[5 12]

$$\alpha_{ij} = -2\bar{\rho}\Delta^2(2\tilde{S_{kl}}\tilde{S_{kl}})^{\frac{1}{2}}\tilde{S_{ij}} \tag{5}$$

where $\tilde{S_{ij}}$ is the filtered strain tensor.

The Ta Phouc Loc model, which is based on the velocity-vorticity (v-ω) formulation of the Navier-Stokes equations. Two spatial filters are used, the first filter denoted by $(^-)$ is used on the fine mesh, and the second 'test filter' denoted by $(\tilde{})$ which is used on the coarse mesh. From eq. (2) we find that

$$\tau_{ij} = \bar{U}_i\bar{U}_j = \overline{U_iU_j} = (\bar{U}_i\bar{U}_j - \overline{\bar{U}_i\bar{U}_j}) - (\overline{\bar{U}_iU_j{}' + U_i{}'\bar{U}_j}) - \overline{U_i{}'U_j{}'} \tag{6}$$

where the fluctuations are defined as $U_i{}' = U_i - \bar{U}_i$.

The turbulent stresses are modeled as

$$\tau_{ij} = v_t\left(\frac{\partial \bar{U}_i}{\partial x_j} + \frac{\partial \bar{U}_j}{\partial x_i}\right) - \frac{2}{3}k\delta_{ij} \tag{7}$$

The eddy viscosity v_t is determined by the mixed-scale turbulence model introduced by L.Ta Phouc[13]

$$v_t = C|\bar{\omega}|^\alpha k^{(1-\alpha)/2}\Delta^{(1+\alpha)} \tag{8}$$

where ω is the vorticity, $\Delta = (\Delta_x\Delta_y\Delta_z)^{\frac{1}{3}}$ is an average grid size, k is the turbulent kinetic energy, α is a parameter which takes a value between 0 and 1. From a previous study[14] it was found that the model performs best when $\alpha = 0.5$.

The turbulent kinetic energy is estimated from the test filter $(\tilde{})$ as

$$k = \frac{1}{2}\sum_{j=1}^{3}(U_j - \bar{U}_j)^2 \approx \frac{1}{2}\sum_{j=1}^{3}\left(\bar{U}_j - \tilde{\bar{U}}_j\right)^2 \tag{9}$$

where U_j is the unfiltered velocity field and $\tilde{\bar{U}}_j$ is the doubled filtered velocity field obtained by applying the second filter on the resolved velocity $\bar{U}_j$.[13 14 15]

2.2 COMPUTATIONAL DOMAIN AND RESULTS

The computational domain is shown in Fig. 1 and consists of an inlet section (swirl generator), a cylinder and an outlet section. At the inlet of the computational domain a uniform radial and tangential velocity is defined and at the outlet a zero-gradient boundary condition is applied.

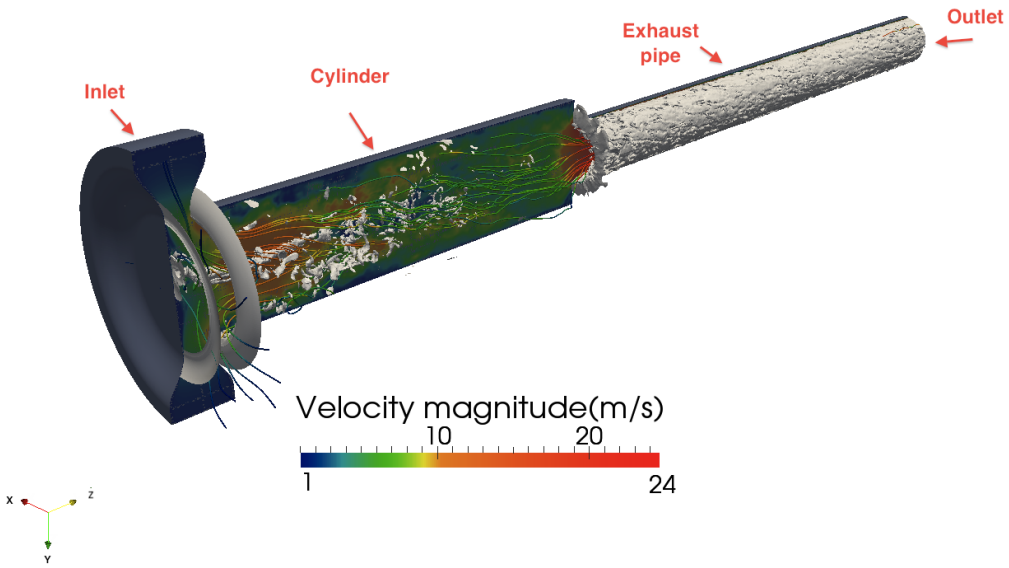

(a)

Figure 1: 3D cross sectional view showing the velocity magnitude, vorticity contours (in white) and streamlines.

The results shown in Fig. 2 show that generally there is a good agreement between computational and experimental particle image velocimetry (PIV) results that have been measured previously[4]. The models capture the wake and jet like profiles of the axial velocity but both are not as pronounced as in the experimental results.

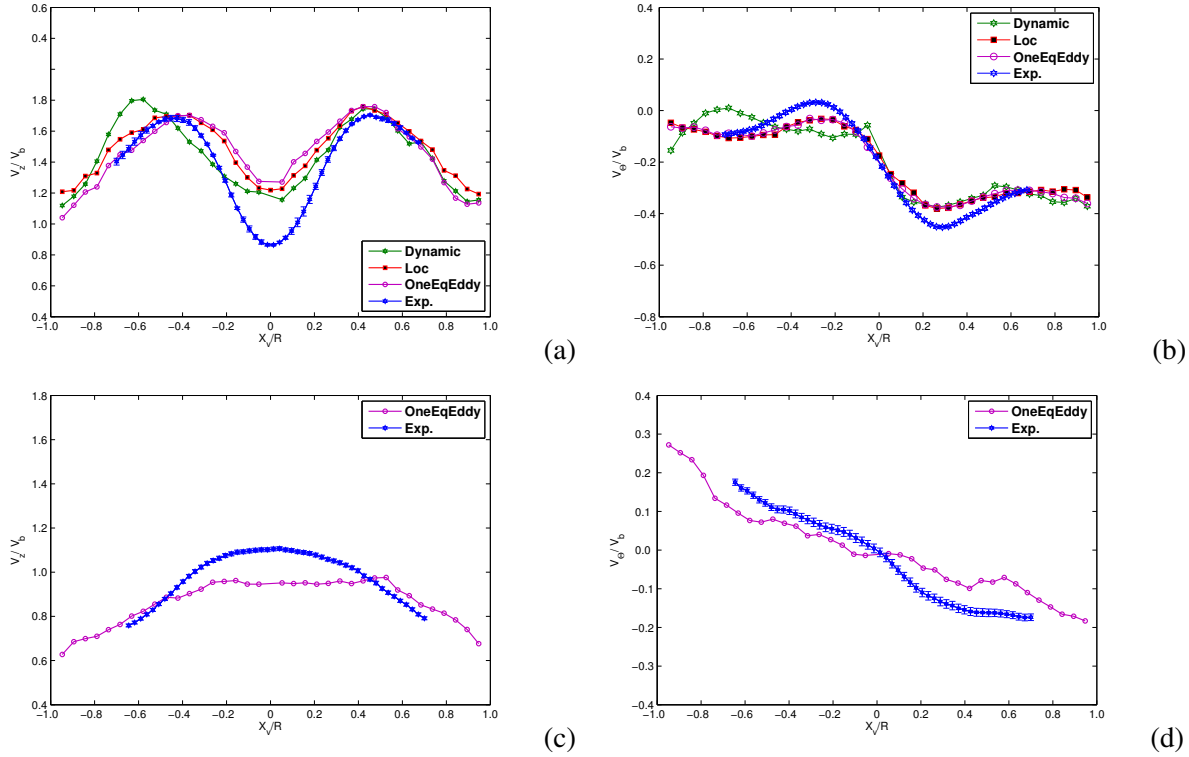

Figure 2: (a) (c) Time averaged axial velocity profiles for the 100%,50% open ports, (b) (d) Time averaged tangential velocity profiles for the 100%,50% open ports, at the axial position $z/D = 2.016$

REFERENCES

[1] Kitoh, S. Experimental Study of turbulent swirling flow in a straight pipe. *J. Fluid Mech.* **225**, 445–479 (1991).

[2] Algifri, A. H., Bhadwaj, R. K. & Rao, Y. V. N. Turbulence Measurements in Decaying Swirl Flow in a Pipe. *Applied Scientific Research* **45**, 233–250 (1988).

[3] Escudier, M. P., Bornstein, J. & Maxworthy, T. The dynamics of confined vortices. *Mathematical and Physical Sciences* **382**, 335–360 (1982).

[4] Haider, S. *Experimental and Numerical Study of Swirling Flow in Scavenging Process for 2-Stroke Marine Diesel Engines*. Ph.D. thesis, Technical University of Denmark (2010).

[5] Wang, P. *Large Eddy simulation of Turbulent Swirling Flows and Turbulent Premixed Combustion*. Ph.D. thesis, Lund Institute of Technology (2005).

[6] Dejoan, A., Jang, Y. J. & Leschziner, M. A. Comparative LES and Unsteady RANS Computation for a Periodically-Perturbed Separated Flow over a Backward-Facing Step. *Fluids Eng.* **127**, 872–879x (2005).

[7] Narasimhamurthy, V. *Unsteady RANS simulation of Turbulent Trailing-Edge Flow*. Ph.D. thesis, Chalmers University of Technology (2004).

[8] Wegner, B., Schneider, C., Dreizler & Janicka, J. Assessment of unsteady RANS in predicting swirl flow instability based on LES and experiments. *Int. J. Heat Fluid Flow* **25**, 528–536 (2004).

[9] Wang, P. & Bai, X. S. Large eddy simulation and experimental studies of a confined turbulent swirling flow. *Phys. Fluids* (2004).

[10] Lesieur, M., Metais, O. & Comte, P. *Large Eddy Simulations of Turbulence* (Cambridge University Press, 2005).

[11] Moene, A. F. *Swirling pipe flow with axial strain Experiment and Large Eddy Simulation*. Ph.D. thesis, Technische Universiteit Eindhoven (2003).

[12] Germano, M., Piomelli, U., Moin, P. & Cabot, W. H. A dynamic subgrid-scale eddy viscosity model. *Phys. Fluids* **3**, 1760–1765 (1991).

[13] Tenaud, C., Pellerin, S., Dulieu, A. & Phouc, L. T. Large Eddy simulations of spatially developing incompressible 3D mixing layer using the $v - \omega$ formulation. *Computers & Fluids* **34**, 67–96 (2005).

[14] Shen, W. Z., Zhu, W. & Sorensen, J. N. Aeroacoustic computations for turbulent airfoil flows. *AIAA* **47** (2009).

[15] Sagaut, P. *Large Eddy Simulation for Incompressible Flows* (Springer), 3 edn.